NTIA Report 83-124

Further Investigations of the Multiple Knife-Edge Attenuation Function

L.E. Vogler

U.S. DEPARTMENT OF COMMERCE
Malcom Baldrige, Secretary

Susan G. Stuebing, Acting Assistant Secretary
for Communications and Information

May 1983

TABLE OF CONTENTS

LIST OF FIGURES

FURTHER INVESTIGATIONS OF THE MULTIPLE KNIFE-EDGE ATTENUATION FUNCTION

L. E. Vogler*

The multiple knife-edge (MKE) attenuation function is derived from Fresnel-Kirchhoff theory and compared with the original derivation from Furutsu's generalized residue series. It is shown that the two methods give complex attenuations with the same absolute magnitude but differing in phase. The analytical basis for an improved computational procedure is developed that eliminates the changeover values and abrupt discontinuities of attenuation inherent in the original MKE computer program. A brief discussion of previous MKE diffraction results is presented and an example comparison is made with the Geometrical Theory of Diffraction and the approximations of Epstein-Peterson and Deygout.

Key words: attenuation calculations; electromagnetic wave propagation; multiple knife-edge diffraction

1. INTRODUCTION

The purpose of this paper is to present further developments concerning the multiple knife-edge (MKE) attenuation function that has been derived recently by Vogler (1981, 1982). The MKE function is the basis for a computer program that calculates attenuation over a propagation path that may consist of up to 10 knife-edges.

The original derivation started from a generalized residue series for diffraction over a sequence of rounded obstacles developed by Furutsu (1963). It is not at all obvious that the MKE function derived in this manner is the same as one derived from Fresnel-Kirchhoff theory such as was used by Millington et al. (1962) for double knife-edge diffraction. In fact, the complex attenuations of the two methods differ in phase although their absolute values are equal. In Section 2 the MKE function will be derived from Fresnel-Kirchhoff theory and an explicit expression for the phase difference factor will be given.

Another aspect to be discussed in the present work concerns the numerical evaluation of the MKE function. Attenuation values are obtained from a series whose terms involve repeated integrals of the error function. As noted in the original

*The author is with the Institute for Telecommunication Sciences, National Telecommunications and Information Administration, U.S. Department of Commerce, Boulder, CO 80303.

paper (Vogler, 1981), certain limitations on the series could cause an abrupt discontinuity in the attenuation as the height of a knife-edge was decreased. In Section 3 an analysis of the problem is presented which leads to a means of eliminating the discontinuities.

2. THE FRESNEL-KIRCHHOFF DERIVATION

The geometry associated with the knife-edge problem is shown in Figure 1. It is assumed that the knife-edges are perfectly absorbing screens placed normal to the direction of propagation and extending to infinity in both horizontal directions and vertically downwards. For a path consisting of N knife-edges and two antenna terminals with heights h_m (above a reference plane) and with separation distances r_m, the diffraction angles θ, for θ_m small, can be approximated by

$$\theta_m = \frac{h_m - h_{m-1}}{r_m} + \frac{h_m - h_{m+1}}{r_{m+1}} = \frac{h_m}{\rho_m^2} - \frac{h_{m-1}}{r_m} - \frac{h_{m+1}}{r_{m+1}} , \qquad (1)$$

where $\rho_m = [r_m r_{m+1}/(r_m + r_{m+1})]^{1/2}$, m=1, 2, ..., N. (2)

In the application of Fresnel-Kirchhoff theory to MKE diffraction, elements of the wavefront are formed in the aperture above each knife-edge and the assumption is made that the field at any particular element arises solely from the total field over the preceding aperture. Only spatial phase change effects are considered significant and the usual condition is made that the separation distances are large compared with the knife-edge heights and wavelength λ. Furthermore, because of knife-edge symmetry in the horizontal direction (y-axis) and because factors obtained by integrating with respect to y cancel out in forming the attenuation (Millington et al., 1962), only phase differences in the plane of propagation are required.

The path length between two points, P and Q, above adjacent knife-edges, m and m+1, minus the distance between knife-edges is

$$\overline{PQ} - r_{m+1} = [r_{m+1}^2 + (X_m - X_{m+1})^2]^{1/2} - r_{m+1} \simeq (X_m - X_{m+1})^2/2r_{m+1} , \qquad (3)$$

where X_m denotes the vertical coordinates of the points.

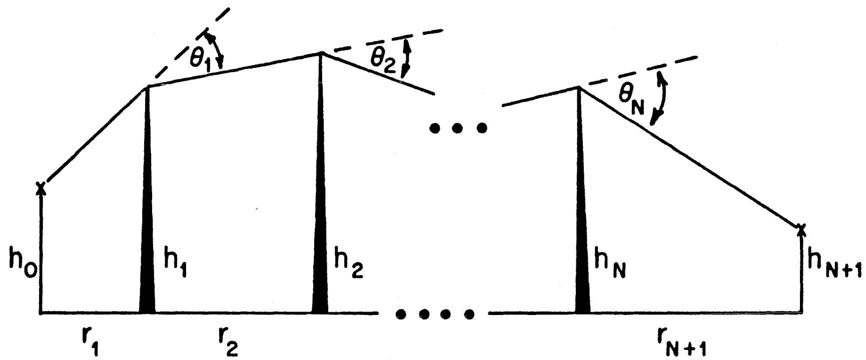

Figure 1. Geometry for multiple knife-edge diffraction.

Assuming plane wave propagation and $\exp(i\omega t)$ time dependence, an element of field strength dE at the receiver due to a particular path from the source can be written as

$$dE \propto \exp[-\hat{F}_N]dX_1 \ldots dX_N \ , \tag{4}$$

where $$\hat{F}_N = \frac{ik}{2}\left[\frac{(h_0-X_1)^2}{r_1} + \sum_{m=1}^{N-1} \frac{(X_m-X_{m+1})^2}{r_{m+1}} + \frac{(X_N-h_{N+1})^2}{r_{N+1}}\right] . \tag{5}$$

Applying Huygens' principle and integrating over each aperture, we find that the total field is then

$$E = K \int_{h_1}^{\infty} \cdot \cdot \cdot \int_{h_N}^{\infty} e^{-\hat{F}_N} dX_1 \cdot \cdot \cdot dX_N \ , \tag{6}$$

where K is an unknown constant.

The free-space field E_0 is found from (6) by allowing the heights h_m to approach $-\infty$. The attenuation relative to the free-space field is then given by

$$(E/E_0) = E(h_m)/E(-\infty) \ , \tag{7}$$

where, for convenience, we have introduced the notation

$$E(h_m) = \int_{h_1}^{\infty} \ldots \int_{h_N}^{\infty} e^{-\hat{F}_N} dX_1 \cdots dX_N \ , \ m = 1, \ \ldots \ , N \ , \tag{8}$$

and $E(-\infty)$ is (8) with the lower limits replaced by $-\infty$.

It appears, that (8) can be integrated in closed form only in certain special cases, one of which is the free-space condition $E(-\infty)$. To show this we first define the function

$$C_k^2 \equiv [r_2 \cdot \ldots r_k R_{k+1}/(r_1+r_2)(r_2+r_3)\ldots(r_k+r_{k+1})]$$

$$= C_{k-1}^2 - \alpha_{k-1}^2 C_{k-2}^2, \ (k \geq 2), \ C_0 \equiv 1, \ C_1 \equiv 1 \ , \tag{9}$$

where $R_{k+1} = r_1 + \cdots + r_{k+1}$, (10)

and $\alpha_m = [r_m r_{m+2}/(r_m+r_{m+1})(r_{m+1}+r_{m+2})]^{1/2} = \rho_m \rho_{m+1}/r_{m+1}$. (11)

Next, we make the change of variables

$$v_m = \left(\frac{ik}{2}\right)^{1/2}\left[\frac{C_m(X_m-h_0)}{C_{m-1}\rho_m} - \frac{C_{m-1}\rho_m(X_{m+1}-h_0)}{C_m r_{m+1}}\right], \quad m = 1, \ldots, N, \tag{12}$$

successively, so that

$$dv_m = (ik/2)^{1/2}(C_m/C_{m-1}\rho_m)dX_m , \tag{13}$$

and with the understanding that $X_{N+1} \equiv h_{N+1}$. Lower limits of the integrals in (8) are given by

$$\upsilon_m = \left(\frac{ik}{2}\right)^{1/2}\left[\frac{C_m(h_m-h_0)}{C_{m-1}\rho_m} - T_m\right], \tag{14a}$$

$$T_m = T_m(v_{m+1}, \ldots, v_N),\ T_N = C_{N-1}\rho_N(h_{N+1}-h_0)/C_N r_{N+1} . \tag{14b}$$

Explicit expressions for υ_m and T_m in terms of knife-edge heights and separation distances are

$$\upsilon_m = (ik/2)^{1/2}\left[(R_{m+1}/r_{m+1}R_m)^{1/2}(h_m-h_0) - T_m\right], \quad m = 1, \ldots, N, \tag{15a}$$

$$T_k = (r_{k+2}R_k/r_{k+1}R_{k+2})^{1/2}\left[(2/ik)^{1/2}v_{k+1} + T_{k+1}\right], \quad k = N-1, \ldots, 1, \tag{15b}$$

$$T_N = (R_N/r_{N+1}R_{N+1})^{1/2}(h_{N+1}-h_0) ,$$

with R_m defined by (10). Notice that $\upsilon_m \to -\infty$ when $h_m \to -\infty$.

With the definitions (12), the function $\hat{F}_N$ becomes

$$\hat{F}_N = v_1^2 + \ldots + v_N^2 + (ik/2)(h_{N+1}-h_0)^2/R_{N+1} \, , \tag{16}$$

where R_{N+1} is the total path distance from source to receiver along the reference plane (see Figure 1). For free-space conditions, (8) is now easily integrated to obtain

$$\begin{aligned} E(-\infty) &\propto \int_{-\infty}^{\infty} \ldots \int_{-\infty}^{\infty} e^{-(v_1^2 + \cdots + v_N^2)} dv_1 \ldots dv_N \\ &= 2^N \left[\int_0^{\infty} e^{-t^2} dt \right]^N = 2^N (\sqrt{\pi}/2)^N = \pi^{N/2} \, , \end{aligned} \tag{17}$$

and the attenuation (7) becomes

$$E/E_0 = (1/\pi)^{N/2} \int_{\upsilon_1}^{\infty} \ldots \int_{\upsilon_N}^{\infty} e^{-(v_1^2 + \ldots + v_N^2)} dv_1 \ldots dv_N \, , \tag{18}$$

where the lower limits are given by (14).

For N=1, (18) is the familiar single knife-edge attenuation function. For N=2 and $h_0=h_3=0$, (18) is equal to the conjugate of the double knife-edge attenuation function given by equation (12) in Millington et al. (1962). The conjugate relationship arises simply because of the different time dependence conventions used.

The Fresnel-Kirchhoff formulation of MKE attenuation is easily expressed in terms of the heights and separation distances of Figure 1 by applying relationships (12) through (14) to equation (18). The result is

$$E/E_0 = (ik/2\pi)^{N/2} (C_N/\rho_1 \ldots \rho_N) e^{\sigma_N''} \int_{h_1}^{\infty} \ldots \int_{h_N}^{\infty} e^{-\hat{F}_N} dX_1 \ldots dX_N \, , \tag{19}$$

where $\sigma_N'' = (ik/2)(h_{N+1}-h_0)^2/R_{N+1}$, (20)

and $\hat{F}_N$, C_N, and ρ_m are defined in (5), (9), and (2) respectively.

The "Fresnel-Kirchhoff" MKE function given by (19) now can be related to the "residue series" MKE function of the original derivation (Vogler, 1981) through the following considerations. First we define the parameter

$$\beta_m = (ik/2)^{1/2}\rho_m\theta_m = (ik/2)^{1/2}\left[\frac{h_m}{\rho_m} - \left(\frac{h_{m-1}}{r_m} + \frac{h_{m+1}}{r_{m+1}}\right)\rho_m\right] . \tag{21}$$

Then with the change of variables

$$x_m = (ik/2)^{1/2}\left[\frac{X_m}{\rho_m} - \left(\frac{h_{m-1}}{r_m} + \frac{h_{m+1}}{r_{m+1}}\right)\rho_m\right], \; m = 1, \ldots, N, \tag{22}$$

we have that

$$dx_m = (ik/2)^{1/2}(dX_m/\rho_m), \; (x_m-\beta_m) = (ik/2)^{1/2}(X_m-h_m)/\rho_m , \tag{23}$$

and the lower limit of the new variable x_m is β_m.

The exponent in (19) now becomes

$$\hat{F}_N - \sigma_N'' = F_N + \sigma_N' - \sigma_N , \tag{24}$$

where $F_N = x_1^2 + \ldots + x_N^2 - 2\sum_{m=1}^{N-1} \alpha_m(x_m-\beta_m)(x_{m+1}-\beta_{m+1})$, (25)

$$\sigma_N' = (ik/2)\left[\sum_{m=1}^{N+1} \frac{(h_{m-1}-h_m)^2}{r_m} - \frac{(h_{N+1}-h_0)^2}{R_{N+1}}\right], \tag{26}$$

$$\sigma_N = \beta_1^2 + \ldots + \beta_N^2 , \tag{27}$$

and α_m and β_m are defined in (11) and (21). Finally, the attenuation in terms of the variables x_m is given by

$$E/E_0 = (1/\pi)^{N/2} C_N e^{\sigma_N - \sigma_N'} \int_{\beta_1}^{\infty} \dots \int_{\beta_N}^{\infty} e^{-F_N} dx_1 \dots dx_N \quad , \tag{28}$$

which is identical to the original derivation obtained from the residue series except for the phase factor $\exp(-\sigma_N')$. (See equation (29) in Vogler (1981).)

The difference in phase arises from the fact that the reference free-space path in the residue series derivation consists of the path segments connecting the tops of the knife-edges, whereas the reference path in the present derivation is the total distance along the reference plane (see Figure 1). It should be noticed that the double knife-edge derivation of Millington et al. (1962) is restricted to the condition that the source and receiver are the same distance from the reference plane (h_0=h_3).

Numerical comparisons of double knife-edge diffraction by the method of Furutsu (1963) and by the method of Millington et al. (1962) show that values of the complex attenuation are the same in absolute value but differ in phase. The phase difference is just the factor $\exp(-\sigma_2')$ where σ_2' is given by (26) with $h_0=h_3=0$.

As a knife-edge tends to $-\infty$, the resultant attenuation should agree both in magnitude and phase with the attenuation that would be calculated without that knife-edge. The use of R_{N+1} as the reference distance for the free-space field assures this result, whereas a reference distance obtained by connecting the tops of the knife-edges does not. Furthermore, in the application of the MKE diffraction to actual radio propagation paths, the geometry of Figure 1 is more convenient than if the reference base were the straight line connecting the tops of the antennnas. Simple expressions that take into account the effects of earth curvature and atmospheric refraction are available to calculate effective heights of terrain features and the receiving antenna relative to the reference plane.

Although the attenuation as given by (19) is in a form more easily recognizable geometrically, the expression in (28) is the one used to obtain numerical evaluations of MKE attenuation. Further discussions on this subject are covered in the next section.

3. ELIMINATION OF CHANGEOVER VALUES

Numerical evaluations of (28) are accomplished by expanding the exponential into a series of terms involving repeated integrals of the error function with arguments β_m. The series forms the basis for a computational algorithm to calculate E/E_0 for arbitrary inputs of knife-edge heights and separation distances and is quite satisfactory for positive or zero β. For negative β the series is still suitable as long as $|\beta|$ is small; however, significant figure loss becomes a problem as any or all β's increase negatively. Here, and in what follows, we shall use the term "negative β" to mean that the angle θ in (21) has a negative value.

The original MKE attenuation computer program calculates attenuation using predetermined, critical values of β. If a knife-edge is sufficiently below the adjacent knife-edges, this results in a negative β that is less than the critical or "changeover" value. That knife-edge is then eliminated and the attenuation is calculated for the remaining knife-edges. The abrupt switch from N to N-1 knife-edges at the changeover value produces a discontinuity in attenuation which, although usually small, prevents a detailed knowledge of variation with height.

Because only negative β's cause problems in the computational procedure, it is of interest to see if the multiple integral can be reformulated into an expression containing only positive (or zero) β's. This may be accomplished in the following manner.

It is assumed that the μ^{th} knife-edge, of height h_μ, is low enough to result in a negative β, β_μ. Then the multiple integral in (19) can be partitioned into

$$\int_{h_1}^{\infty}\cdots\int_{h_\mu}^{\infty}\cdots\int_{h_N}^{\infty} \rightarrow \int_{h_1}^{\infty}\cdots\int_{-\infty}^{\infty}\cdots\int_{h_N}^{\infty} - \int_{h_1}^{\infty}\cdots\int_{-\infty}^{h_\mu}\cdots\int_{h_N}^{\infty} , \tag{29}$$

where, for notational purposes, the first multiple integral on the right hand side will be denoted by I_1 and the second by I_2.

Restricting our attention to I_1, we can write $\hat{F}_N$ from (5) as

$$\hat{F}_N = \left(\frac{ik}{2}\right)\left[\frac{(h_0-X_1)^2}{r_1} + \ldots + \frac{(X_{\mu-1}-X_{\mu+1})^2}{r_\mu+r_{\mu+1}} + \ldots + \frac{(X_N - h_{N+1})^2}{r_{N+1}}\right.$$
$$\left. + \frac{(X_{\mu-1}-X_\mu)^2}{r_\mu} + \frac{(X_\mu-X_{\mu+1})^2}{r_{\mu+1}} - \frac{(X_{\mu-1}-X_{\mu+1})^2}{r_\mu+r_{\mu+1}}\right]$$

$$\equiv \left(\frac{ik}{2}\right) F'_{N-1} + \Omega_\mu , \tag{30}$$

$$\Omega_\mu = \frac{(X_{\mu-1}-X_\mu)^2}{r_\mu} + \frac{(X_\mu - X_{\mu+1})^2}{r_{\mu+1}} - \frac{(X_{\mu-1}-X_{\mu+1})^2}{r_\mu + r_{\mu+1}}$$

$$= \frac{X_\mu{}^2}{\rho_\mu{}^2} - 2\left(\frac{X_{\mu-1}}{r_\mu} + \frac{X_{\mu+1}}{r_{\mu+1}}\right) X_\mu + \frac{X^2_{\mu-1}}{r_\mu} + \frac{X^2_{\mu+1}}{r_{\mu+1}} - \frac{(X_{\mu-1}-X_{\mu+1})^2}{r_\mu + r_{\mu+1}}$$

$$= \left\{\frac{X_\mu}{\rho_\mu} - \left(\frac{X_{\mu-1}}{r_\mu} + \frac{X_{\mu+1}}{r_{\mu+1}}\right)\rho_\mu\right\}^2 . \tag{31}$$

Now make the change of variable

$$v_0 = \left(\frac{ik}{2}\right)^{1/2}\left\{\frac{X_\mu}{\rho_\mu} - \left(\frac{X_{\mu-1}}{r_\mu} + \frac{X_{\mu+1}}{r_{\mu+1}}\right)\rho_\mu\right\},\ dv_0 = \frac{(ik/2)^{1/2}}{\rho_\mu}\ dX_\mu, \tag{32}$$

and I_1 becomes

$$I_1 = \left(\frac{ik}{2\pi}\right)^{N/2}\left(\frac{C_N e^{\sigma''_N}}{\rho_1 \cdots \rho_N}\right)\left\{\left(\frac{2}{ik}\right)^{1/2} \rho_\mu \int_{-\infty}^{\infty} e^{-v_0^2} dv_0\right\} I'_{N-1}$$

$$= (ik/2\pi)^{(N-1)/2} (\rho_\mu C_N/\rho_1 \cdots \rho_N) e^{\sigma''_N} I'_{N-1} , \tag{33}$$

$$\text{where } I'_{N-1} = \int_{h_1}^{\infty} \cdots \int_{h_N}^{\infty} e^{-(ik/2)F'_{N-1}} dX_1 \cdots dX_N , \tag{34}$$

with the understanding that the integral with respect to X_μ has been deleted in (34).

Because of the relationship $(C_N/\rho_1 \cdots \rho_N) = (R_{N+1}/r_1 \cdots r_{N+1})^{1/2}$, it can be seen that (33) is identical to the expression for MKE attenuation (19) over the path if the

μ^{th} knife-edge were absent and an appropriate separation distance of $r_\mu + r_{\mu+1}$ were used. Thus, I_1 can be evaluated as a path with N-1 knife-edges and with the negative β_μ no longer present. The preceding argument will hold for $1 \le \mu \le N$ if we assume, for notational convenience, that $X_0 \equiv h_0$ and $X_{N+1} \equiv h_{N+1}$.

Returning to the second multiple integral in (29), we can apply the change of variables given by (22) to arrive at

$$I_2 = K \int_{\beta_1}^{\infty} \cdots \int_{-\infty}^{\beta_\mu} \cdots \int_{\beta_N}^{\infty} e^{-F_N} \, dx_1 \ldots dx_N$$

$$= K \int_{\beta_1}^{\infty} \cdots \int_{-\beta_\mu}^{\infty} \cdots \int_{\beta_N}^{\infty} e^{-F_N'} \, dx_1 \ldots dx_N \, , \tag{35}$$

$$\text{where } K = (1/\pi)^{N/2} C_N e^{\sigma_N - \sigma_N'} \, , \tag{36}$$

and F_N' is the same as F_N given by (25) except for the linear order terms involving x_μ: the factor $(x_\mu - \beta_\mu)$ is replaced by $(-x_\mu - \beta_\mu) = -(x_\mu + \beta_\mu)$. Since β_μ is negative, the multiple integral in (35) can now be expanded into a series containing repeated integrals of the error function (all with positive arguments) in exactly the same manner as the original computational algorithm. A negative sign, arising from the x_μ integration, will be associated with some of the terms, but the arguments of positive β assure satisfactory convergence.

The partitioning procedure described above can be applied sequentially until no negative β's remain. Thus, any combination of knife-edge heights can be decreased to $-\infty$ and the variation of attenuation studied. An algorithm utilizing partitioning will eliminate the sudden discontinuities of attenuation that occur in the original MKE computer program; however, a disadvantage is that increased computer time is sometimes necessary because of the extra number of multiple integrals that must be evaluated. Of course if all β's are positive, there is no difference in running time. Furthermore, in the basic series used to calculate the attenuation, fewer terms are necessary to assure a given accuracy if all β's are positive rather than some being negative. Thus, partitioning, which guarantees positive β's, will have more multiple integrals but each one will need fewer terms for evaluation. For this reason partitioning when N<7 is often more advantageous as far as computer running time is concerned.

The partition method has been incorporated into a computer program that calculates MKE attenuation for inputs of up to 10 knife-edges. This unpublished program (designated PAMKE) allows detailed study of attenuation even in the interference regions. Comparisons of the output from PAMKE with attenuations as calculated from the original computer program (also unpublished and designated FAMKE) that made use of changeover values are shown in the following examples.

A propagation path consisting of four knife-edges arranged as shown in Figure 2 is assumed. It should be remembered that the knife-edge heights are measured from an arbitrary reference level and that it is their relative heights that are of interest. The MKE attenuation, (E/E_0) in dB, as a function of receiver height, h_R in meters, is plotted for both PAMKE (with partitions) and FAMKE (with changeover values). As the receiver rises from the shadow region into line-of-sight, the solid curve (PAMKE) shows small oscillations caused by interference from the intervening knife-edges. At larger heights, beyond the range of the figure, the curve eventually levels off at A(dB)=0 as it should.

The output from FAMKE, represented by the dashed lines, show the discontinuities in attenuation that occur when a changeover point is reached and a knife-edge is eliminated. A changeover value of $\beta_{min} = -1$ was selected for this example. The attenuations from the two programs are the same until h_R = 20m, at which point the fourth knife-edge (h_4 = 10m) is eliminated resulting in $\sim$0.5dB difference in the outputs of the two programs. The FAMKE curve is not shown from h_R = 25m to h_R = 47m because it is practically the same as the solid curve. At h_R = 47m the third knife-edge is eliminated, and at h_R = 67m the second is eliminated. The effective number of knife-edges, N_{eff}, is the number used by FAMKE over each portion of the curve. At no point is the difference in attenuations greater than 1dB.

Another example giving a comparison of the two algorithms is shown in Figure 3. In this case a propagation path consisting of five evenly spaced knife-edges (separation distances = 2km) is assumed. The heights are varied simultaneously such that the diffraction angles θ at all of the knife-edges are equal in value. A frequency, f=1908.538 MHz, was assumed, this value being chosen simply for computational convenience.

When clusters of negative θ's occur, it is sometimes difficult to determine changeover values that will assure enough significant figures being retained in the calculations entering into FAMKE. For this reason a test on the convergence of the series is also included, and if the test fails, the knife-edge with the "most negative" β is eliminated.

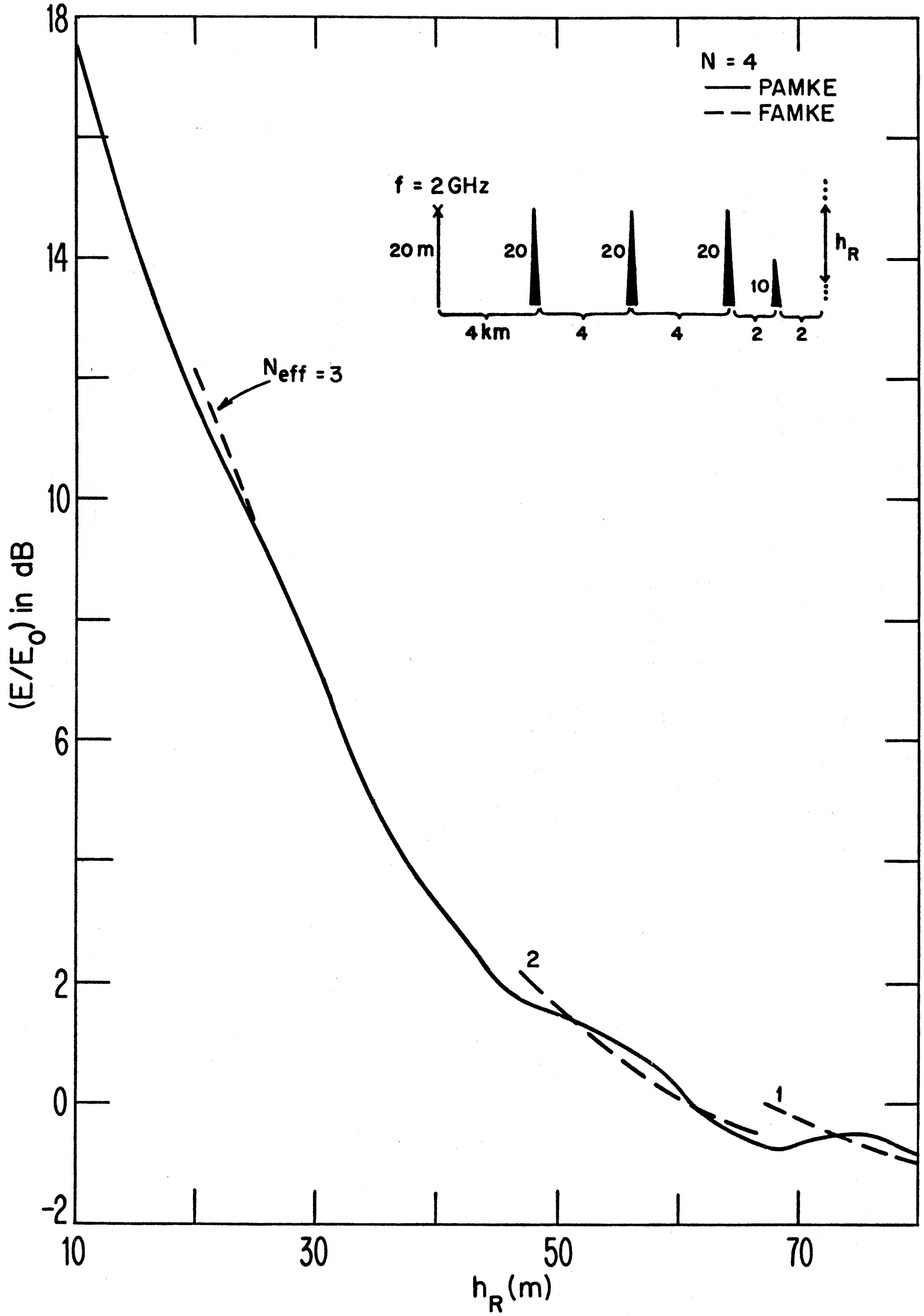

Figure 2. Comparison of attenuation by programs FAMKE and PAMKE for a four knife-edge path as receiver height is varied.

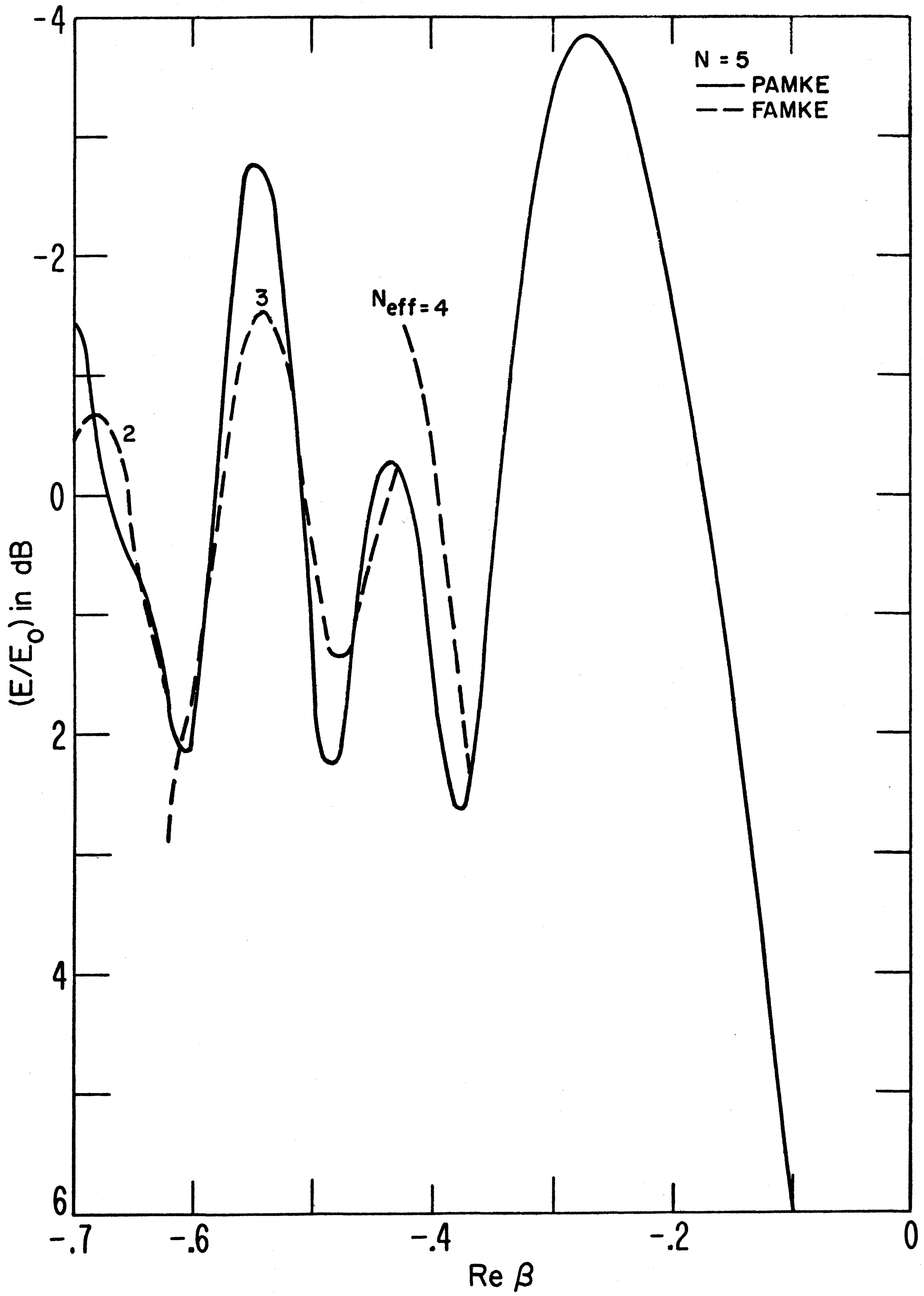

Figure 3. Comparison of attenuation by programs FAMKE and PAMKE for a five knife-edge path in which all θ's are equal.

In Figure 3 the outputs of PAMKE and FAMKE are the same for Reβ >-0.37. At this point the convergence test fails and FAMKE then calculates the attenuation for one less knife-edge (the portion of the dashed curve labeled N_{eff} = 4). Similar failures occur at -0.42 and -0.62, resulting in the discontinuities at these values. It can be seen that differences in attenuation from the exact curve as calculated by PAMKE are always less than 1.5 dB.

The partitioning procedure described in this section provides a means of calculating the MKE attenuation function (equation (28)) for any knife-edge heights without concern for the problems of discontinuities or significant figure loss. Details of attenuation variation even in the interference region can thus be shown for any combination of knife-edges.

4. DISCUSSION

The derivation of the MKE function by Fresnel-Kirchhoff theory as used in this paper implies certain restrictive conditions regarding the physics of the problem, e.g., perfectly absorbing half-screens, plane wave propagation, kr>>1, and path difference approximations. However, as a mathematical function, its numerical evaluation may be accomplished even when the geometric parameters (h and r) tend to unrealistic physical values. For instance the use of partitioning provides valid answers for any knife-edge heights subject only to computer limitations. With regard to separation distances, the limitations are more inherent in the computational algorithm.

Mathematically, the MKE function can be evaluated for separation distances ranging from zero to infinity. This is apparent when closed form solutions of the function are available. For example, Vogler (1982) has derived the attenuation for three knife-edges under the condition $\theta_1=\theta_2=\theta_3=0$:

$$E/E_0 = (1/8)[1+(2/\pi)\ \tan^{-1}a_1 + \tan^{-1}a_2 + \tan^{-1}a_3\ ], \tag{37}$$

$$a_1 = [r_1(r_3+r_4)/r_2r_t]^{1/2},\ a_2 = [(r_1+r_2)r_4/r_3r_t]^{1/2}\ ,$$

$$a_3 = [r_1r_4/(r_2+r_3)r_t]^{1/2}\ ,\ r_t = r_1+r_2+r_3+r_4\ .$$

For r_2 or r_3 = 0, (37) reduces to the known expression for a double knife-edge. For r_2 and r_3 = 0, (E/E_0)=1/2 which is the value for a single knife-edge.

When $r_2=r_3$ and r_1, r_4 take on various combinations of zero and infinity, (37) gives the same values as obtained from formulas in Lee (1978). In that paper the MKE attenuation for general N is derived under the conditions: all $\theta_i \equiv 0$; $r_2, \ldots, r_N$ = constant (r_0, say); and r_1, r_{N+1} = 0 or ∞. Six cases are given which prove useful in helping to determine the validity of the computation series in the MKE computer program. The factor C_N (see equation (9)) is included in each case for purposes of later discussion.

Case (1): $r_1, r_{N+1} \to \infty$;

$$E/E_0 \sim 1/2, \; C_N \sim 0. \tag{38a}$$

Case (2): $r_1 \to \infty, r_{N+1} \to 0$ or $r_1 \to 0, r_{N+1} \to \infty$;

$$E/E_0 \sim \frac{1}{2}\,\frac{1\cdot3\cdot5\cdots(2N-3)}{2\cdot4\cdot6\cdots(2N-2)}, \; C_N \sim (1/2^{N-2})^{1/2} . \tag{38b}$$

Case (3): $r_1 = r_0, r_{N+1} \to 0$ or $r_1 \to 0, r_{N+1} = r_0$;

$$E/E_0 \sim 1/2N, \; C_N \sim (N/2^{N-1})^{1/2} . \tag{38c}$$

Case (4): $r_1, r_{N+1} \to 0$;

$$E/E_0 \sim 1/4(N-1), \; C_N \sim [(N-1)/2^{N-2}]^{1/2} . \tag{38d}$$

Case (5): $r_1, r_{N+1} = r_0$;

$$E/E_0 \sim 1/(N+1), \; C_N = [(N+1)/2^N]^{1/2} . \tag{38e}$$

Case (6): $r_1 \to \infty, r_{N+1} = r_0$ or $r_1 = r_0, r_{N+1} \to \infty$;

$$E/E_0 \sim \frac{1\cdot3\cdot5\cdots(2N-1)}{2\cdot4\cdot6\cdots(2N)}, \; C_N \sim (1/2^{N-1})^{1/2} . \tag{38f}$$

Comparisons of attenuation for N=10 as calculated from (38) and as calculated from program PAMKE are shown in Table 1. The values used in PAMKE when r_1, r_{11} approached 0 or ∞ were 10^{-9} or 10^8, respectively; in all cases r_0 was set equal to unity.

Table 1. Attenuation Comparisons for N=10

Case	E/Eo(equat.(38))	E/Eo(PAMKE)	C_{10}
(1)	0.5000	$\sim$0	0
(2)	0.09274(20.66dB)	0.08639(21.27dB)	0.0625
(3)	0.05000(26.02dB)	0.04998(26.02dB)	0.1398
(4)	0.02778(31.13dB)	0.02778(31.13dB)	0.1875
(5)	0.09091(20.83dB)	0.09076(20.84dB)	0.1036
(6)	0.1762(15.08dB)	0.1551(16.19dB)	0.0442

The maximum number of series terms (160) was used in all cases for the PAMKE calculations. When C_N is close to zero, this number of terms is insufficient to provide a valid answer. In cases (2) and (6) the result is good to about one significant figure; however, in cases (3), (4), and (5) PAMKE gives three or more significant figures.

The factor C_N Provides a good indication as to how closely the series calculation approaches the correct answer. Table 1 suggests (and other studies tend to verify) that for $C_N \gtrsim 0.1$, the attenuation is good to about 0.1 dB or better; as C_N ranges below 0.1, the accuracy becomes poorer. Note that the C_N in (38) increase as N decreases, which should result in better accuracy. Cases (2) and (6) were run for N's such that C_N=0.125 in each case. For case (2) (N=8), PAMKE gave (E/E_0)=0.1037 as against an exact value of 0.1047; for case (6) (N=7), PAMKE gave (E/E_0)=0.2073 versus the exact value 0.2095. The difference in dB in each case is about 0.09 dB.

The condition, all θ's=0, is a "worst case" situation as far as series convergence within a set number of terms is concerned. This is because repeated integrals of the error function decrease rapidly as the argument β increases, and fewer terms are required to assure a given number of significant figures. This fact, combined with the partitioning procedure, means that the relationship, $C_N \gtrsim 0.1$, provides a fairly conservative accuracy test for PAMKE when applied to most propagation paths.

If each and every diffraction angle θ_i is large enough such that every β_i>>1, then the attenuation is well approximated by the first term of the series expansion derived in the original MKE paper:

$$E/E_0 \sim 2^{-N} C_N e^{\sigma_N - \sigma_N'} \prod_{i=1}^{N} \mathrm{erfc}(\beta_i) , \tag{39}$$

where erfc(z) is the complementary error function as defined in Abramowitz and Stegun (1964;p.297). Since $\beta_i \gg 1$ for i=1,...,N, $\mathrm{erfc}(\beta_i)$ may be replaced by the first term of its asymptotic expansion and (39) then becomes

$$\begin{aligned} E/E_0 &\sim (2\sqrt{\pi})^{-N} C_N e^{-\sigma_N'}/\beta_1 \cdots \beta_N \\ &= e^{-\sigma_N'} (i2\pi k)^{-N/2} (R_{N+1}/r_1 \cdots r_{N+1})^{1/2}/\theta_1 \cdots \theta_N , \end{aligned} \tag{40}$$

where R_{N+1} denotes the total path distance, σ_N' is defined in (26), and use has been made of (2), (9), (21), and (27).

Equation (40) is of interest in that it may also be obtained from the Geometrical Theory of Diffraction (GTD). If the knife-edge configuration is such that each edge lies well into the shadow region of the preceding knife-edge, the GTD diffracted field can be expressed as the product of functions of the form

$$f(s) = s^{-1/2} e^{-iks} , \tag{41a}$$

$$D(\varepsilon,\delta) = (2\sqrt{2\pi k})^{-1} \left[\csc\left\{(\delta+\varepsilon)/2\right\} \pm \sec\left\{(\delta-\varepsilon)/2\right\}\right] e^{-i\pi/4} . \tag{41b}$$

In the above, s is the slant distance to the edge, ε and δ are the elevation angles as measured from the horizontal to the top of the knife-edge at the source and at the field point, respectively, and the plus or minus signs in the Keller diffraction coefficient D correspond to vertical or horizontal polarization (Keller, 1962).

Since $(\varepsilon+\delta)=\theta$, the diffracted field u_d for a single knife-edge according to the GTD is

$$\begin{aligned} u_d &= f(s_1) D(\theta_1) f(s_2) \\ &\sim (e^{-iks_1}/\sqrt{s_1}) \left[\sqrt{i2\pi k}\, \theta_1\right]^{-1} (e^{-iks_2}/\sqrt{s_2}) , \end{aligned} \tag{42}$$

where the approximate expression is valid for

$$0 \ll \theta_1 \text{ and } \theta_1 \simeq \sin \theta_1 \quad . \tag{43}$$

In the case of multiple knife-edges, the diffracted field is the product of functions, $D(\theta_i)f(s_{i+1})$:

$$u_d = f(s_1)D(\theta_1)f(s_2) \ \ldots \ D(\theta_N)f(s_{N+1})$$
$$\sim (i2\pi k)^{-N/2} e^{-ik(s_1 + \ \ldots \ + s_{N+1})} \left\{ (s_1 \ldots s_{N+1})^{1/2} \theta_1 \ldots \theta_N \right\}^{-1} , \tag{44}$$

$$0 \ll \theta_i \text{ and } \theta_i \simeq \sin \theta_i, \ i = 1, \ \ldots, \ N. \tag{45}$$

For a reference free-space field, $R_{N+1}^{-1/2}\exp(-ikR_{N+1})$, and assuming $s_i \simeq r_i$ except in the phase term where use is made of the approximation in (3), we see that the GTD attenuation obtained from (44) is identical to (40).

Two widely used approximations to MKE diffraction have been suggested by Epstein and Peterson (1953) and by Deygout (1966). Both approximations consist simply of products of single knife-edge attenuation functions, the difference being in the way the "source" and "receiver" of each knife-edge are determined. If we designate the single knife-edge function as given in (28) by: $A_s(\beta)=(1/2)\text{erfc}(\beta)$, the Epstein-Peterson ($A_{EP}$) and Deygout ($A_D$) approximations can be expressed as

$$A_{EP} = \prod_{m=1}^{N} A_s(\beta_m) \ , \ A_D = \prod_{m=1}^{N} A_s(\beta'_m) \ , \tag{46}$$

where β_m is defined in (21) and β'_m has the same form but with the distances and diffraction angle θ'_m determined from Deygout's "principle mask" method.

Pogorzelski (1982) has pointed out that, under the conditions (45) where the GTD equation (40) is valid, A_{EP} has the same θ dependence but the r and the phase dependence differs; A_D has the same r and phase dependence but the θ dependence is different. Thus, asymptotic expressions for the two approximations are

$$A_{EP} \sim e^{-\sigma_N}(i2\pi k)^{-N/2}F_{EP}(r)/\theta_1 \cdots \theta_N , \tag{47a}$$

$$F_{EP}(r) = \begin{cases} [(r_1+r_2)\cdots(r_N+r_{N+1})/r_1(r_2\cdots r_N)^2 r_{N+1}]^{1/2} & , N \geq 2 \\ 1/\rho_1 & , N = 1 \end{cases}$$

$$A_D \sim e^{-\sigma_N'}(i2\pi k)^{-N/2}F_D(r)/\theta_1'\cdots\theta_N' , \tag{47b}$$

$$F_D(r) = [R_{N+1}/r_1\cdots r_{N+1}]^{1/2} .$$

The difference in dB between the approximations and (40), assuming (45), can be written as

$$(A_{EP})_{dB} \sim (E/E_o)_{dB} - 20\log(1/C_N) , \tag{48a}$$

$$(A_D)_{dB} \sim (E/E_o)_{dB} + 20\log(K_1 \ldots K_N) , \tag{48b}$$

$$\theta_m' = K_m\theta_m, \; m=1,\ldots,N.$$

Figure 4 compares some of the attenuation formulas discussed in this section. The propagation path is the same as that assumed for Figure 3, i.e., five evenly spaced knife-edges with heights simultaneously varying such that all θ's are equal to the same value. The attenuation in dB is plotted versus this value, θ in mrad, for the MKE function (from program PAMKE), the GTD (from equation (40)), and the two approximations from (46), A_{EP} and A_D.

As expected, the MKE and GTD give the same result for $\theta \gtrsim 0.015$ rad. Of course, for very large θ the two curves begin to diverge, with the GTD being exact and the MKE an approximation. For θ decreasing to zero, no GTD formula for five knife-edges exists at the present time and the approximation of (40) is not valid in this region. In fact at θ=0, the attenuation has the value, -20 log(1/6)=15.56dB (see equation (38e)), whereas (40) goes to $-\infty$.

The Epstein-Peterson and Deygout approximations both have the value 5(6.02)=30.1dB at θ=0, which exceeds the exact value by 14.5dB. When $\theta \gg 0$, A_{EP} and A_D approach constant differences from the exact curve as is indicated in (48). For A_{EP} the difference is 20 log(1/C_5)=7.27dB; for A_D the difference is equal to 20 log[3(3/2)(3/2)]=16.6dB.

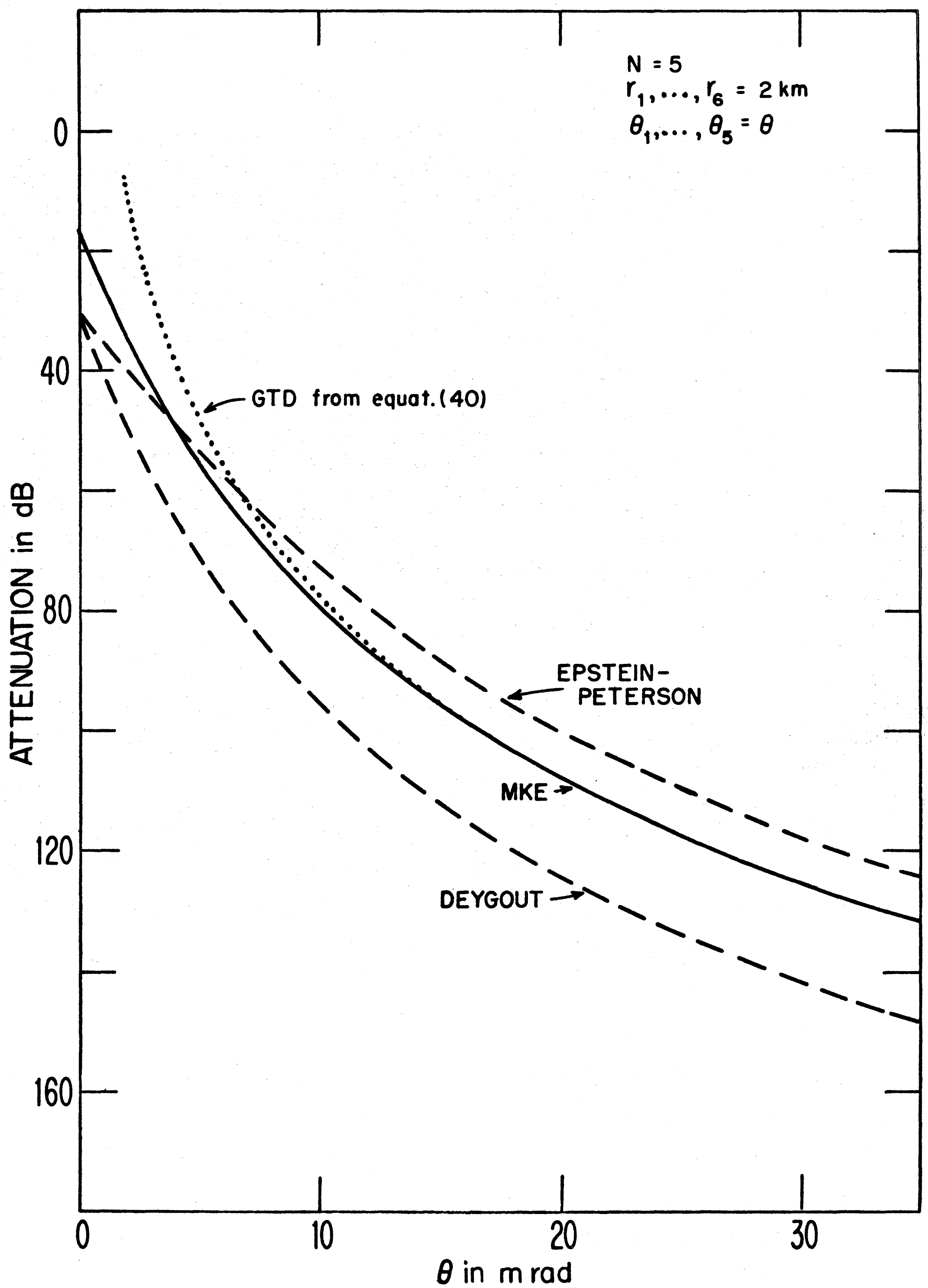

Figure 4. Attenuation for the same five knife-edge path as in Figure 3 (all θ's equal). Comparisons are shown for MKE, GTD, and the approximations of Epstein-Peterson and of Deygout.

5. SUMMARY

Fresnel-Kirchhoff theory has been used to derive an expression for attenuation caused by multiple knife-edge diffraction assuming plane wave propagation over perfectly absorbing half planes. The complex attenuation derived in this manner differs from that derived from Furutsu's generalized residue series only in the phase, the phase difference factor being given explicitly in (28). This phase difference arises from the fact that the reference free-space path in the residue series consists of the path segments joining the tops of the knife-edges, whereas the Fresnel-Kirchhoff reference path is the straight line distance from source to receiver locations.

An improved computational procedure based on the partitioning of multiple integrals has been developed. The integrals are partitioned as in (29) until all the arguments of the repeated integrals of the error function are positive, which eliminates problems of retaining significant figures when negative arguments are involved. The key step in the analysis is to show that the multiple integral containing the limit going from $-\infty$ to $+\infty$ is exactly the expression for the MKE attenuation over the path with one less knife-edge. This is demonstrated in (33) and the related equations. Comparisons of results from a computer program using partitioning (PAMKE) with the original program (FAMKE) are presented in Figures 2 and 3.

Finally, in section 4 results of other approaches to the MKE diffraction problem are presented and their relationship to the MKE attenuation function of this paper is discussed. In particular, it is shown that the first term of the MKE series expansion reduces to the Geometrical Theory of Diffraction (GTD) solution for certain ranges of the diffraction angles θ (see equations (40) and (44)). Other solutions considered include Lee's formulas, (38), and the approximations of Epstein-Peterson and of Deygout, (46).

6. REFERENCES

Abramowitz, M., and I.A. Stegun (1964), Handbook of Mathematical Functions, National Bureau of Standards, AMS 55.

Deygout, J. (1966), Multiple knife-edge diffraction of microwaves, IEEE Trans. Ant. Prop. AP-14, pp. 480-489.

Epstein, J., and D.W. Peterson (1953), An experimental study of wave propagation at 850 Mc, Proc. IRE 41, pp. 595-611.

Furutsu, K. (1963), On the theory of radio wave propagation over inhomogeneous earth, J. Res. NBS (Rad.Prop.) 67D, pp. 39-62.

Kellar, J.B. (1962), Geometrical Theory of Diffraction, J. Opt. Soc. Amer. 52, pp. 116-130.

Lee, S.W. (1978), Path integrals for solving some electromagnetic edge diffraction problems, J. Math. Phys. 19, pp. 1414-1422.

Millington, G., R. Hewitt, and F.S. Immirzi (1962), Double knife-edge diffraction in field-strength predictions, Proc. IEE, Monograph No. 507E, pp. 419-429.

Pogorzelski, R.J. (1982), A note on some common diffraction link loss models, Radio Sci. 17, pp. 1536-1540.

Vogler, L.E. (1981), The attenuation of electromagnetic waves by multiple knife-edge diffraction, NTIA Report 81-86. (Available as PB82-139239, Natl. Tech. Inf. Serv., Springfield, Va.).

Vogler, L.E. (1982), An attenuation function for multiple knife-edge diffraction, Radio Sci. 17, pp. 1541-1546.

FORM **NTIA-29**
(4-80)

U.S. DEPARTMENT OF COMMERCE
NAT'L. TELECOMMUNICATIONS AND INFORMATION ADMINISTRATION

BIBLIOGRAPHIC DATA SHEET

	1. PUBLICATION NO.	2. Gov't Accession No.	3. Recipient's Accession No.
	NTIA Report 83-124		

4. TITLE AND SUBTITLE
Further Investigations of the Multiple Knife-Edge Attenuation Function

5. Publication Date
May 1983

6. Performing Organization Code
NTIA/ITS

7. AUTHOR(S)
L. E. Vogler

9. Project/Task/Work Unit No.
910 4142

8. PERFORMING ORGANIZATION NAME AND ADDRESS
U.S. Department of Commerce
National Telecomm. and Information Administration
Institute for Telecommunication Sciences
325 Broadway, Boulder, CO 80303

10. Contract/Grant No.

11. Sponsoring Organization Name and Address
National Security Agency
9800 Savage Road
Fort George Meade, MD 20755

12. Type of Report and Period Covered
NTIA Report

13.

14. SUPPLEMENTARY NOTES

15. ABSTRACT *(A 200-word or less factual summary of most significant information. If document includes a significant bibliography or literature survey, mention it here.)*

The multiple knife-edge MKE attenuation function is derived from Fresnel-Kirchhoff theory and compared with the original derivation from Furutsu's generalized residue series. It is shown that the two methods give complex attenuations with the same absolute magnitude but differing in phase. The analytical basis for an improved computational procedure is developed that eliminates the changeover values and abrupt discontinuities of attenuation inherent in the original MKE computer program. A brief discussion of precious MKE diffraction results is presented and an example comparison is made with the Geometrical Theory of Diffraction and the approximations of Epstein-Peterson and Deygout.

16. Key Words *(Alphabetical order, separated by semicolons)*

attenuation calculations; electromagnetic wave propagation; multiple knife-edge diffraction

17. AVAILABILITY STATEMENT	18. Security Class. *(This report)*	20. Number of pages
☒ UNLIMITED.	Unclassified	23
☐ FOR OFFICIAL DISTRIBUTION.	19. Security Class. *(This page)* Unclassified	21. Price:

☆U.S. GOVERNMENT PRINTING OFFICE: 1983—679-744/352